Numerical experiments on plasma focus neon soft x-ray scaling

2009 Plasma Phys. Control. Fusion 51 105013

(http://iopscience.iop.org/0741-3335/51/10/105013)

Plasma Phys. Control. Fusion **51** (2009) 105013 (8pp) doi:10.1088/0741-3335/51/10/105013

Numerical experiments on plasma focus neon soft x-ray scaling

S Lee[1,2,3], S H Saw[3], P Lee[2] and R S Rawat[2]

[1] Institute for Plasma Focus Studies, 32 Oakpark Drive, Chadstone, VIC3148, Australia
[2] NSSE, National Institute of Education, Nanyang Technological University, Singapore 637616, Singapore
[3] INTI University College, 71800 Nilai, Malaysia

E-mail: leesing@optusnet.com.au

Received 25 February 2009, in final form 1 August 2009
Published 21 September 2009
Online at stacks.iop.org/PPCF/51/105013

Abstract

Numerical experiments are carried out systematically to determine the neon soft x-ray yield Y_{sxr} for optimized neon plasma focus with storage energy E_0 from 0.2 kJ to 1 MJ. The ratio $c = b/a$, of outer to inner electrode radii, and the operating voltage V_0 are kept constant. E_0 is varied by changing the capacitance C_0. Parametric variation at each E_0 follows the order operating pressure P_0, anode length z_0 and anode radius a until all realistic combinations of P_0, z_0 and a are investigated. At each E_0, the optimum combination of P_0, z_0 and a is found that produces the biggest Y_{sxr}. At low energies the soft x-ray yield scales as $Y_{sxr} \sim E_0^{1.6}$ whilst towards 1 MJ it becomes $Y_{sxr} \sim E_0^{0.8}$. The Y_{sxr} scaling laws are found to be $Y_{sxr} \sim I_{peak}^{3.2}$ (0.1–2.4 MA) and $Y_{sxr} \sim I_{pinch}^{3.6}$ (0.07–1.3 MA) throughout the range investigated. When numerical experimental points with other c values and mixed parameters are included, there is evidence that the Y_{sxr} versus I_{pinch} scaling is more robust and universal, remaining unchanged whilst the Y_{sxr} versus I_{peak} scaling changes slightly, with more scatter becoming evident.

1. Introduction

Plasma focus machines operated in neon have been studied as intense sources of soft x-rays (SXRs) with potential applications [1–3]. Whilst many recent experiments have concentrated efforts on low energy devices [1–3] with a view of operating these as repetitively pulsed sources, other experiments have looked at x-ray pulses from larger plasma focus devices [4, 5] extending to the megajoule regime. However, numerical experiments simulating x-ray pulses from plasma focus devices are gaining more interest in the public domain. For example, the Institute of Plasma Focus Studies [6] conducted a recent International Internet Workshop on Plasma Focus Numerical Experiments [7], at which it was demonstrated that the Lee model code [8] not only computes realistic focus pinch parameters, but also absolute values of SXR yield Y_{sxr} which are consistent with those measured experimentally. A comparison was made

for the case of the NX2 machine [3], showing good agreement between computed and measured Y_{sxr} as a function of P_0 [7, 9]. This gives confidence that the Lee model code gives realistic results in the computation of Y_{sxr}. In this paper, we report on a comprehensive range of numerical experiments with storage energies E_0 in the range 0.2 kJ–1 MJ in order to derive the scaling laws for plasma focus neon Y_{sxr}, in terms of E_0, peak discharge current I_{peak} and focus pinch current I_{pinch}.

Numerical experiments for deriving scaling laws on neutron yield Y_n have already been reported [10, 11]. These have shown that in terms of storage energy E_0, $Y_n \sim E_0^2$ at small E_0 of kilojoules, the scaling 'slowing' with increasing E_0, becoming $Y_n \sim E_0$ in the higher energy ranges of megajoules. In terms of I_{peak}, a single power law covers the scaling, this being $Y_n \sim I_{peak}^{3.8}$; likewise another single power law for I_{pinch}, this being $Y_n \sim I_{pinch}^{4.5}$. These scaling laws apply from kJ to 25 MJ with corresponding I_{peak} from 0.1 to 5.7 MA and I_{pinch} from 0.08 to 2.4 MA. It needs to be stressed that these scaling rules only apply to optimized operational points. It also needs to be pointed out that the distinction of I_{pinch} from I_{peak} is of basic importance [12–14]. The scaling with I_{pinch} is the more fundamental and robust one, since obviously there are situations (no pinching or poor pinching however optimized) where I_{peak} may be large but Y_n is zero or small, whereas the scaling with I_{pinch} is certainly more consistent with all situations. In these works the primary importance of I_{pinch} for scaling plasma focus properties including neutron yield Y_n has been firmly established [10–14].

This primary importance of I_{pinch} has been borne in mind in our numerical experiments on neon plasma focus. In the context of neon Y_{sxr} scaling, not much work appears to have been reported in the literature. Gates, in optimization studies, had proposed [15] that the total energy emitted as x-rays may scale as $Y_x \sim I_{peak}^4/(\text{pinchradius})^2$. This scaling rule is not very useful for predictive purposes since for a given capacitor bank whilst I_{peak} may be estimated, the focus pinch radius is difficult to quantify. Moreover if one considers a certain gas, say, neon, then for an optimum operation one really needs to fix an axial speed, in which case the speed factor $S = (I_{peak}/a)/P_0^{0.5}$ (where a is the anode radius and P_0 is the operating pressure)is fixed [16]. Moreover for optimum operation in neon, the pinch radius has a fixed relationship to a [17]. This means that the Gates scaling rule reduces to $Y_x \sim P_0 I_{peak}^2$. In this context, it is of greater interest to note that Filippov *et al* [5] had compared the experimental data of two Filippov-type plasma focus operated at 0.9 MJ and 5 kJ, respectively, and on the basis of the experimental results of just these two machines had proposed a scaling for the K-shell lines of neon $Y_x \sim I_{pinch}^{3.5–4}$. They further stated that such a scaling is in conformity to the resistive heating mechanism of neon plasma. It is unlikely that Filippov's $Y_x \sim I_{pinch}^{3.5–4}$ is compatible with Gates' $Y_x \sim I_{peak}^4/(\text{pinchradius})^2$. It is against this background of rather scanty experimental data that our numerical experiments are designed to comprehensively cover the range of E_0 from 0.2 kJ to 1 MJ using the Lee model code which models the Mather-type configurations.

2. The Lee model code for neon SXR yields

The Lee model couples the electrical circuit with plasma focus dynamics, thermodynamics and radiation, enabling realistic simulation of all gross focus properties. This approach focusing on gross properties is different from magnetohydrodynamic (MHD) codes where spatially resolved and detailed description of plasma properties is calculated. Many authors have developed and used MHD and fluid models of the plasma focus. Behler and Bruhns [18] developed a 2D three-fluid code. Garanin and Mamyshev [19] introduced the MHD model, which takes into account anomalous resistivity. However, none of these studies [18–23] has

resulted in published data on SXR yields, nor any comparison with laboratory experiments on SXR yields [18–23].

Our basic model, described in 1984 [24], was successfully used to assist several projects [25–27]. Radiation-coupled dynamics was included in the five-phase code leading to numerical experiments on radiation cooling [28]. The vital role of a finite small disturbance speed discussed by Potter in a Z-pinch situation [29] was incorporated together with real gas thermodynamics and radiation-yield terms. Before this 'communication delay effect' was incorporated, the model consistently over-estimated the radial speeds by a factor of ∼2 and shock temperatures by a factor ∼4. This version, using the 'signal-delay slug', which became a must-have feature in all subsequent versions, assisted other research projects [30–33] and was web-published in 2000 [34] and 2005 [35]. Plasma self-absorption was included in 2007 [34] improving SXR yield simulation. The code has been used extensively in several machines including UNU/ICTP PFF [25, 28, 30, 31, 36–38], NX2 [3, 32, 33], NX1 [2, 3] and adapted for the Filippov-type plasma focus DENA [39]. A recent development is the inclusion of the neutron yield, Y_{n}, using a beam–target mechanism [10, 11, 13, 40, 41], incorporated in recent versions [8] of the code (later than RADPFV5.13), resulting in realistic Y_{n} scaling with I_{pinch} [10, 11]. The versatility and the utility of the model are demonstrated in its clear distinction of I_{pinch} from I_{peak} [12] and the recent uncovering of a plasma focus pinch current limitation effect [13, 14]. The description, theory, code and a broad range of results of this 'Universal Plasma Focus Laboratory Facility' are available for download from [8].

In the code, neon line radiation Q_{L} is calculated as follows:

$$\frac{\mathrm{d}Q_{\mathrm{L}}}{\mathrm{d}t} = -4.6 \times 10^{-31} n_i^2 Z Z_n^4 (\pi r_{\mathrm{p}}^2) z_{\mathrm{f}} / T,$$

where for the temperatures of interest in our experiments we take $Y_{\mathrm{sxr}} = Q_{\mathrm{L}}$.

Hence the SXR energy generated within the plasma pinch depends on the following properties: number density n_i, effective charge number Z, pinch radius r_{p}, pinch length z_{f}, temperature T and pinch duration, since in our code Q_{L} is obtained by integrating over the pinch duration.

This generated energy is then reduced by the plasma self-absorption which depends primarily on density and temperature; the reduced quantity of energy is then emitted as the SXR yield. It was first pointed out by Mahe [37] that a temperature around 300 eV is optimum for SXR production. Bing's subsequent work [32] and our experience through numerical experiments suggest that around 2×10^6 K (below 200 eV) or even a little lower seems to be better in providing the best mix of helium-like and hydrogen-like neon ions radiating SXR lines in the spectral range 1–1.3 nm. Hence unlike the case of neutron scaling, for SXR scaling there is an optimum small range of temperatures (T window) in which to operate.

3. Numerical experiments and their results

We use the Lee model code to carry out a series of numerical experiments over the energy range 0.2 kJ–1 MJ. For the neon operation, the Lee model code had previously been designed to compute the line radiation yield. For this work we want to distinguish that part of the line yield that is SXRs. Reviewing previous experimental and numerical work by Mahe [37] and more detailed numerical work by Bing [32], we are able to fix a temperature range for neon at which the radiation is predominantly SXR coming from He-like and H-like neon ions. Bing, in particular, carried out a line-by-line computation using a corona method and computed the relative intensities of each of the four neon SXR lines (He- and H-like) as functions of temperature. From this paper we set the following temperature range: 2.3–5.1 $\times 10^6$ K as that

Table 1. Optimized configuration found for each E_0. Optimization carried out with RESF = 0.1, $c = 1.5$, $L_0 = 30$ nH and $V_0 = 20$ kV and model parameters f_m, f_c, f_{mr}, f_{cr} are fixed at 0.06, 0.7, 0.16 and 0.7, respectively. The v_a, v_s and v_p are the peak axial, radial shock and radial piston speeds, respectively.

E_0 (kJ)	C_0 (μF)	a (cm)	z_0 (cm)	P_0 (Torr)	I_{peak} (kA)	I_{pinch} (kA)	v_a (cm μs^{-1})	v_s (cm μs^{-1})	v_p (cm μs^{-1})	Y_{sxr} (J)	Efficiency (%)
0.2	1	0.58	0.5	4.0	100	68	5.6	22.5	14.9	0.44	0.2
1	5	1.18	1.5	4.0	224	143	6.6	23.3	15.1	7.5	0.8
2	10	1.52	2.1	4.0	300	186	6.8	23.6	15.2	20	1.0
6	30	2.29	5.2	4.2	512	294	8.1	24.5	15.6	98	1.6
10	50	2.79	7.5	4.0	642	356	8.7	24.6	15.7	190	1.9
20	100	3.50	13	4.0	861	456	9.6	24.6	16.0	470	2.4
40	200	4.55	20	3.5	1 109	565	10.3	24.7	16.2	1 000	2.5
100	500	6.21	42	3.0	1 477	727	11.2	24.8	16.4	2 700	2.7
200	1 000	7.42	63	3.0	1 778	876	11.4	24.8	16.5	5 300	2.7
400	2 000	8.70	98	3.0	2 079	1 036	11.4	24.9	16.5	9 400	2.4
500	2 500	9.10	105	2.9	2 157	1 086	11.5	25.1	16.7	11 000	2.2
1 000	5 000	10.2	160	3.0	2 428	1 261	11.4	25.2	16.7	18 000	1.8

relevant to the production of neon SXRs. In any shot, for the duration of the focus pinch, whenever the focus pinch temperature is within this range, the line radiation is counted as neon SXRs. Whenever the pinch temperature is outside this range, the line radiation is not included as neon SXRs.

The following parameters are kept constant: (i) the ratio $b = c/a$ (kept at 1.5, which is practically optimum according to our preliminary numerical trials), (ii) the operating voltage V_0 (kept at 20 kV), (iii) static inductance L_0 (kept at 30 nH, which is already low enough to reach the I_{pinch} limitation regime [13, 14] over most of the range of E_0 we are covering) and (iv) the ratio of stray resistance to surge impedance, RESF (kept at 0.1). The model parameters [7, 8, 10–14] f_m, f_c, f_{mr}, f_{cr} are also kept at fixed values of 0.06, 0.7, 0.16 and 0.7.

The storage energy E_0 is changed by changing the capacitance C_0. Parameters that are varied are operating pressure P_0, anode length z_0 and anode radius a. Parametric variation at each E_0 follows the order P_0, z_0 and a until all realistic combinations of P_0, z_0 and a are investigated. At each E_0, the optimum combination of P_0, z_0 and a is found that produces the biggest Y_{sxr}. In other words at each E_0, a P_0 is fixed, a z_0 is chosen and a is varied until the largest Y_{sxr} is found. Then keeping the same values of E_0 and P_0, another z_0 is chosen and a is varied until the largest Y_{sxr} is found. This procedure is repeated until for that E_0 and P_0, the optimum combination of z_0 and a is found. Then keeping the same value of E_0, another P_0 is selected. The procedure for parametric variation of z_0 and a as described above is then carried out for this E_0 and new P_0 until the optimum combination of z_0 and a is found. This procedure is repeated until for a fixed value of E_0, the optimum combination of P_0, z_0 and a is found.

The procedure is then repeated with a new value of E_0. In this manner after systematically carrying out some 2000 runs, the optimized runs for various energies are tabulated in table 1. From the data of table 1, we plot Y_{sxr} against E_0 as shown in figure 1.

Figure 1 shows that Y_{sxr} scales as $E_0^{1.6}$ at low energies in the 0.2 to several kJ region. The scaling 'drops' as E_0 is increased and Y_{sxr} scales as $E_0^{0.76}$ at high energies towards 1 MJ.

We then plot Y_{sxr} against I_{peak} and I_{pinch} and obtain figure 2

Figure 2 shows that the yield scales as $Y_{sxr} \sim I_{pinch}^{3.6}$ and $Y_{sxr} \sim I_{peak}^{3.2}$. The I_{pinch} scaling has less scatter than the I_{peak} scaling.

We next test the scaling when the fixed parameters RESF, c, L_0 and V_0 and model parameters f_m, f_c, f_{mr}, f_{cr} are varied. We add in the results of some numerical experiments

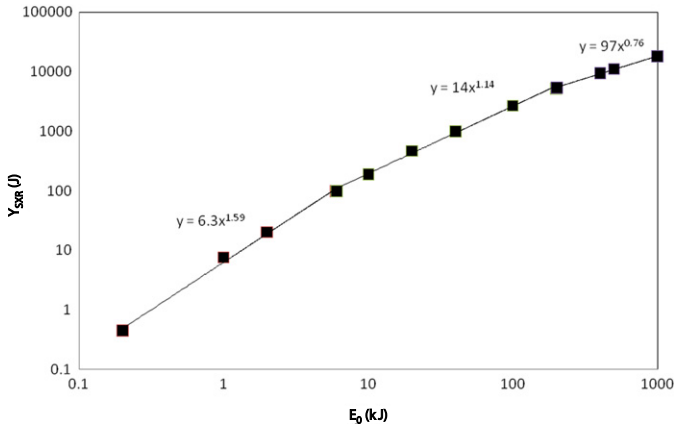

Figure 1. Y_{sxr} versus E_0. The parameters kept constant are: RESF $= 0.1$, $c = 1.5$, $L_0 = 30$ nH and $V_0 = 20$ kV and model parameters f_m, f_c, f_{mr}, f_{cr} at 0.06, 0.7, 0.16 and 0.7, respectively.

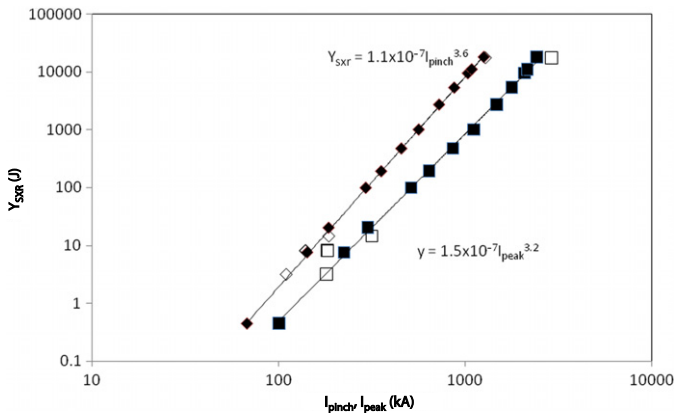

Figure 2. Y_{sxr} versus I_{pinch}, I_{peak}. The parameters kept constant for the black data points are RESF $= 0.1$, $c = 1.5$, $L_0 = 30$ nH and $V_0 = 20$ kV and model parameters f_m, f_c, f_{mr}, f_{cr} at 0.06, 0.7, 0.16 and 0.7, respectively. The white data points are for specific machines which have different values for the parameters c, L_0 and V_0.

using the parameters of several existing plasma focus devices including the UNU/ICTP PFF (RESF $= 0.2$, $c = 3.4$, $L_0 = 110$ nH and $V_0 = 14$ kV with fitted model parameters $f_m = 0.05$, $f_c = 0.7$, $f_{mr} = 0.2$, $f_{cr} = 0.8$) [6–8, 37], the NX2 (RESF $= 0.1$, $c = 2.2$, $L_0 = 20$ nH and $V_0 = 11$ kV with fitted model parameters $f_m = 0.06$, $f_c = 0.7$, $f_{mr} = 0.16$, $f_{cr} = 0.7$) [6–9, 32] and PF1000 (RESF $= 0.1$, $c = 1.39$, $L_0 = 33$ nH and $V_0 = 27$ kV with fitted model parameters $f_m = 0.1$, $f_c = 0.7$, $f_{mr} = 0.15$, $f_{cr} = 0.7$) [6–8, 13]. These new data points (white data points in figure 2) contain wide ranges of c, V_0, L_0 and model parameters. The resulting Y_{sxr} versus I_{pinch} log–log curve remains a straight line, with the scaling index 3.6 unchanged and with no more scatter than before. However, the resulting Y_{sxr} versus I_{peak} curve now exhibits considerably larger scatter and the scaling index has changed.

Another way of looking at the comparison of the I_{pinch} scaling and the I_{peak} scaling is to consider some unoptimized cases, e.g. at very high or very low pressures. In these cases, Y_{sxr} is zero and I_{pinch} is zero but there is a value for I_{peak}. This is an argument that the I_{pinch} scaling is more robust. However, it must be noted that both scalings are applicable only to optimized

points. Nevertheless, noting that the $Y_{sxr} \sim I_{pinch}$ scaling has less scatter than the $Y_{sxr} \sim I_{peak}$ scaling particularly when mixed-parameter cases are included, the conclusion is that the I_{pinch} scaling is the more universal and robust one.

4. Discussion of results

The numerical experiments with neon plasma focus over the storage energy range of 0.2 kJ–1 MJ show that within the stated constraints of these experiments, scaling with E_0 is $Y_{sxr} \sim E_0^{1.6}$ in the low energy range towards sub kJ and 'decreases' to $Y_{sxr} \sim E_0^{0.8}$ in the high energy range investigated towards 1 MJ. A single power law applies for the I_{peak} scaling: $Y_{sxr} \sim I_{peak}^{3.2}$, in the range 0.1–2.4 MA; likewise for I_{pinch} scaling: $Y_{sxr} \sim I_{pinch}^{3.6}$, in the range 0.07–1.3 MA. The observation of the numerical experiments, bolstered by fundamental considerations, is that the I_{pinch} scaling is the more universal and robust one. It may also be worth noting that our comprehensively surveyed numerical experiments for Mather configurations in the range of energies 1 kJ–1 MJ produce an I_{pinch} scaling rule not compatible with Gates' rule [15]. However, it is remarkable that our I_{pinch} scaling index of 3.6, obtained through a set of comprehensive numerical experiments over a range of 0.2 kJ–1 MJ, on the Mather-type devices is within the range 3.5–4 postulated on the basis of sparse experimental data (basically just two machines one at 5 kJ and the other at 0.9 MJ) by Filippov [5], for Filippov configurations in the range of energies 5 kJ–1 MJ.

It must be pointed out that the results represent scaling for comparison with baseline plasma focus devices that have been optimized in terms of electrode dimensions. It must also be emphasized that the scaling with I_{pinch} works well even when there are some variations in the actual device from $L_0 = 30$ nH, $V_0 = 20$ kV and $c = 1.5$. However, there may be many other parameters which can change which could lead to a further enhancement of x-ray yield. For example, 100 J SXR yields have been reported for the 2–3 kJ devices NX1 [3] and NX2+ [33]. The enhancement in yield in those cases may be due to an enhanced I_{pinch}, which may in turn be due to an insulator sleeve arrangement which organizes a good initial breakdown; NX1 has a special high dielectric constant insulator sleeve and NX2+ has an insulator sleeve geometry instead of the insulator disc geometry of NX2 [3]. On the other hand, the yield enhancement could also be due to the anode shape since NX1 is rounded, with specially shaped anode and cathode, and NX2+ is tapered, which may cause changes in the plasma parameters, e.g. plasma density even at the same I_{pinch}. The explanation for x-ray yield enhancement being due to a change in plasma density when tapering the anode is supported by the Lee code [8] and computed by Wong *et al* [33]. Some examples of experimental techniques which may enhance x-ray yields are changing the anode shape, changing the insulator sleeve material, pre-ionization of the ambient gas, pre-ionization of the insulator sleeve, introduction of gas mixture, introduction of density variations in the plasma focus tube by gas puffing (both at the insulator and at the anode tip), changing the insulator sleeve length and thus the plasma sheath curvature, varying the operating voltage, changing the cathode geometry and changing the anode material. Some of these experimental variations may yield significant changes in f_m, f_c, f_{mr}, f_{cr} while others might not be easily simulated by the Lee model in its current form.

5. Conclusions

In conclusion, this paper has shown that within the scope of this paper, neon x-ray yields scale well with $Y_{sxr} = 1.07 \times 10^{-7} I_{pinch}^{3.63}$ (where yield is in joules and current in kiloamperes). This

implies that for applications requiring high x-ray yield, the plasma focus must be designed to optimize I_{pinch}. For example from table 1, it can be seen that the optimum efficiency for SXR yield is with a capacitor bank energy of 100 kJ. One factor may be that beyond 100 kJ, I_{pinch} does not increase well with bank energy due to the increase in the impedance of the plasma focus in comparison with that of the bank impedance. Therefore for larger devices, it may be necessary to operate at a higher voltage and use higher driver impedance to ensure increasing x-ray yield efficiency beyond 100 kJ. Based on the scaling law proposed here, it is possible to classify experimental yield enhancements into three categories: (i) 'compensating for unoptimized focus' where experiments start off with a focus showing unexpectedly low yield, i.e. below the scaling law and then the yield is 'enhanced' by techniques other than changing of anode dimensions to follow the scaling law, (ii) 'increasing I_{pinch}' for example by reducing the current shedding or increasing the current by current stepping with novel driver circuits where the enhanced device still follows the same scaling law and (iii) 'new regime of operation' where plasma parameters such as density, dimensions and lifetime are changed at the same I_{pinch} and yield is beyond the scaling law.

References

[1] Kato Y and Be S H 1986 *Appl. Phys. Lett.* **48** 686
[2] Bogolyubov E P *et al* 1998 *Phys. Scr.* **57** 488–94
[3] Lee S, Lee P, Zhang G, Feng X, Gribkov V A, Mahe L, Serban A and Wong T K S 1998 *IEEE Trans. Plasma Sci.* **26** 1119
[4] Filippov N V *et al* 1996 *IEEE Trans Plasma Sci.* **24** 1215–23
[5] Filippov N V, Filippova T I, Khutoretskaia I V, Mialton V V and Vinogradov V P 1996 *Phys. Lett.* A **211** 168–171
[6] Institute for Plasma Focus Studies http://www.plasmafocus.net
[7] 2008 *Internet Workshop on Plasma Focus Numerical Experiments (IPFS-IBC1) (14 April–19 May 2008)* http://www.plasmafocus.net/IPFS/Papers/IWPCAkeynote2ResultsofInternet-basedWorkshop.doc
[8] Lee S *Radiative Dense Plasma Focus Computation Package: RADPF* http://www.intimal.edu.my/school/fas/UFLF/File1RADPF.htm; http://www.plasmafocus.net/IPFS/modelpackage/File1RADPF.htm
[9] Lee S, Rawat R S, Lee P and Saw S H 2009 *J. Appl. Phys.* **106** 023309
[10] Lee S and Saw S H 2008 *J. Fusion Energy* **27** 292–5
[11] Lee S 2008 *Plasma Phys. Control. Fusion* **50** 105005
[12] Lee S, Saw S H, Lee P C K, Rawat R S and Schmidt H 2008 *Appl. Phys. Lett.* **92** 111501
[13] Lee S and Saw S H 2008 *Appl. Phys. Lett.* **92** 021503
[14] Lee S, Lee P, Saw S H and Rawat R S 2008 *Plasma Phys. Control. Fusion* **50** 065012
[15] Gates D C 1983 *Proc. 2nd Int. Conf. on Energy Storage, Compression and Switching (Venice, Italy, 1978)* vol 2 (New York: Plenum) p 329
[16] Lee S and Serban A 1996 *IEEE Trans. Plasma Sci.* **24** 1101
[17] Lee S 1998 Scaling of the plasma focus *Int. Workshop on Plasma Focus Research (PF98) (Kudowa, Poland, July 1998)* http://eprints.ictp.it/109/ (also in *1st Conf. on Plasma Physics Applications (Julich, Germany, 2004)* (*International Cooperation Bilateral Seminars* vol 34) (Julich: Forschungszentrum Julich Gmbh) pp 27–33)
[18] Behler K and Bruhns H 1987 *Phys. Fluids* **30** 3767
[19] Garanin S F and Mamyshev V I 2008 *Plasma Phys. Rep.* **34** 639–49
[20] Potter D E 1971 *Phys. Fluids* **14** 1911 doi:10.1063/1.1693700
[21] Vikhrev V, Ivanov V V and Rosanova G A 1993 *Nucl. Fusion* **33** 311
[22] Stepniewski W 2006 *J. Phys.: Conf. Ser.* **44** 215–220 doi:10.1088/1742-6596/44/1/031 (*1st Int. Workshop and Summer School on Plasma Physics (IWSSPP'05) (Kiten, Bulgaria, 8–12 June 2005)*)
[23] Yordanov V, Ivanova–Stanik I and Blagoev A 2006 *J. Phys.: Conf. Ser.* **44** 215–20 doi:10.1088/1742-6596/44/1/031 (*1st Int. Workshop and Summer School on Plasma Physics (IWSSPP'05) (Kiten, Bulgaria, 8–12 June 2005)*)
[24] Lee S 1984 Plasma focus model yielding trajectory and structure *Radiations in Plasmas* vol II ed B McNamara (Singapore: World Scientific) ISBN 9971-966-37-9 pp 978–87
[25] Lee S *et al* 1988 *Am. J. Phys.* **56** 62
[26] Tou T Y, Lee S and Kwek K H 1989 *IEEE Trans. Plasma Sci.* **17** 311
[27] S Lee 1991 *IEEE Trans. Plasma Sci.* **19** 912

[28] Ali J b 1990 Development and studies of a small plasma focus *PhD Thesis* Universiti Teknologi Malaysia, Malaysia
[29] Potter D E 1978 *Nucl. Fusion* **18** 813–23
[30] Lee S and Serban A 1998 *J. Plasma Phys.* **60** 3–15
[31] Liu M H, Feng X P, Springham S V and Lee S 1998 *IEEE Trans. Plasma Sci.* **26** 135–40
[32] Bing S 2000 Plasma dynamics and x-ray emission of the plasma focus *PhD Thesis* NIE ICTP Open Access Archive: http://eprints.ictp.it/99/
[33] Wong D, Lee P, Zhang T, Patran A, Tan T L, Rawat R S and Lee S 2007 *Plasma Sources Sci. Technol.* **16** 116–23
[34] Lee S 2000–2007 http://ckplee.myplace.nie.edu.sg/plasmaphysics/
[35] Lee S 2005 ICTP Open Access Archive: http://eprints.ictp.it/85/
[36] Lee S 1998 *Twelve Years of UNU/ICTP PFF—A Review* IC 98 (231) Abdus Salam ICTP, Miramare, Trieste; ICTP OAA: http://eprints.ictp.it/31/
[37] Mahe L 1996 Soft x-rays from compact plasma focus *PhD Thesis* Nanyang Technological University Singapore. ICTP Open Access Archive: http://eprints.ictp.it/327/
[38] Saw S H, Lee P, Rawat R S and Lee S 2009 *IEEE Trans. Plasma Sci.* **37** 1276–82
[39] Siahpoush V, Tafreshi M A, Sobhanian S and Khorram S 2005 *Plasma Phys. Control. Fusion* **47** 1065
[40] Gribkov V A *et al* 2007 *J. Phys. D: Appl. Phys.* **40** 3592
[41] Springham S V, Lee S and Rafique M S 2000 *Plasma Phys. Control. Fusion* **42** 1023